© 2016. Published by The Company of Biologists Ltd | Development (2016) 143, 318-328 doi:10.1242/dev.127860

RESEARCH ARTICLE

Prox1 and fibroblast growth factor receptors form a novel regulatory loop controlling lens fiber differentiation and gene expression

Dylan S. Audette[1], Deepti Anand[1], Tammy So[2], Troy B. Rubenstein[1], Salil A. Lachke[1,3], Frank J. Lovicu[2] and Melinda K. Duncan[1,*]

ABSTRACT

Lens epithelial cells differentiate into lens fibers (LFs) in response to a fibroblast growth factor (FGF) gradient. This cell fate decision requires the transcription factor Prox1, which has been hypothesized to promote cell cycle exit in differentiating LF cells. However, we find that conditional deletion of *Prox1* from mouse lenses results in a failure in LF differentiation despite maintenance of normal cell cycle exit. Instead, RNA-seq demonstrated that Prox1 functions as a global regulator of LF cell gene expression. Intriguingly, Prox1 also controls the expression of fibroblast growth factor receptors (FGFRs) and can bind to their promoters, correlating with decreased downstream signaling through MAPK and AKT in *Prox1* mutant lenses. Further, culturing rat lens explants in FGF increased their expression of Prox1, and this was attenuated by the addition of inhibitors of MAPK. Together, these results describe a novel feedback loop required for lens differentiation and morphogenesis, whereby Prox1 and FGFR signaling interact to mediate LF differentiation in response to FGF.

KEY WORDS: Lens, Morphogenesis, Regulatory loop

INTRODUCTION

Tissue morphogenesis requires cell-cell communication, often mediated by growth factors, that reprograms cellular phenotypes. This response is fine-tuned by regulation of growth factor receptor expression, allowing cells to respond to, or ignore, specific stimuli (Cross and Dexter, 1991; Scata et al., 1999). These processes can be studied in the ocular lens as cells differentiate in response to growth factor signaling, and the simplicity of this tissue makes it an ideal model with which to study the resulting morphological and molecular changes (Lovicu et al., 2011).

The lens arises from an area of head ectoderm termed the lens placode, which invaginates to form the lens vesicle (LV) (Streit, 2004). The anterior hemisphere of the LV retains its epithelial morphology, while the posterior cells extend anteriorly and terminally differentiate into primary lens fibers (LFs) (Bhat, 2001). This process requires fibroblast growth factor (FGF), which is secreted by the developing retina and binds to fibroblast growth factor receptors (FGFRs) expressed by lens cells (de Iongh and Duncan, 2015; Lovicu et al., 2011). Although FGFRs are required for LF differentiation (Zhao et al., 2008) and are upregulated in differentiating LFs (de Iongh et al., 1997), the regulation of these receptors remains undefined.

LF differentiation also requires the transcription factors cMaf (Kim et al., 1999), Sox1 (Nishiguchi et al., 1998) and Prox1 (Wigle et al., 1999), as mice mutant for any of these genes never form LFs. Prox1 is a sequence-specific DNA-binding transcription factor that is defined by its conserved, atypical homeodomain (Chen et al., 2008; Tomarev et al., 1996). Although Prox1 is first detected in the lens placode (Duncan et al., 2002), eyes lacking Prox1 develop normally until the posterior LV cells fail to elongate into LFs (Wigle et al., 1999). Although it has been proposed that Prox1 regulation of cell cycle exit drives this phenotype (Wigle et al., 1999), other mutants with cell cycle exit defects do not phenocopy the *Prox1* null lens (Fromm et al., 1994; Zhang et al., 1998). Here, we further investigate the cause of the LF cell morphogenesis failure observed in *Prox1* mutant mice.

RESULTS

Mice with lens-specific deletion of *Prox1* phenocopy the lens morphology of *Prox1* null mice

As *Prox1* null mice die *in utero* (Wigle and Oliver, 1999), $Prox1^{flox/flox}$*MLR10Cre+* (*Prox1* cKO) mice were generated that inactivate *Prox1* in lens. *Prox1* cKO lenses develop normally prior to E11.5; however, whereas the primary LFs of wild-type (WT) mice elongate by E12.5 (Fig. 1A) and stain vibrantly with Eosin, this does not occur in *Prox1* cKO lenses (Fig. 1D). Secondary LF differentiation begins in WT by E13.5 (Fig. 1B,C). By contrast, most *Prox1* cKO lenses do not exhibit LF elongation and never stain intensely with Eosin (Fig. 1E,F).

Prox1 protein is located in the nuclei of differentiating LFs at E12.5 (Fig. 1G) and is maintained at the transition zone of E13.5 and E15.5 WT lenses (Fig. 1H,I). Prox1 protein levels are unaltered at E11.5 in *Prox1* cKO LV (not shown), are substantially reduced at the posterior of *Prox1* cKO lenses by E12.5 (Fig. 1J), and are below the limit of detection at E13.5 and E15.5 (Fig. 1K,L).

Prox1 cKO LFs exit the cell cycle appropriately and do not undergo robust apoptosis

Since *Prox1* mutant lens phenotypes have been hypothesized to result from cell cycle exit failure in the posterior LV (Wigle et al., 1999), we evaluated DNA synthesis and cell cycle exit. In WT mice, cells undergoing DNA synthesis are confined to the lens epithelium at E13.5 (Fig. 2A,A′). Similarly, only the most anterior cells of *Prox1* cKO LVs exhibit detectable DNA synthesis (Fig. 2B,B′). Cell cycle exit coincident with LF cell differentiation is preceded by elevated expression of the cell cycle inhibitors (CKIs) $p27^{Kip1}$ and $p57^{Kip2}$ (Cdkn1b and Cdkn1c – Mouse Genome Informatics)

[1]Department of Biological Sciences, University of Delaware, Newark, DE 19716, USA. [2]Discipline of Anatomy & Histology, Bosch Institute & Save Sight Institute, University of Sydney, Sydney, New South Wales 2000, Australia. [3]Center for Bioinformatics and Computational Biology, University of Delaware, Newark, DE 19716, USA.

*Author for correspondence (duncanm@udel.edu)

Received 7 July 2015; Accepted 26 November 2015

Development (2016) 143, 318-328 doi:10.1242/dev.127860

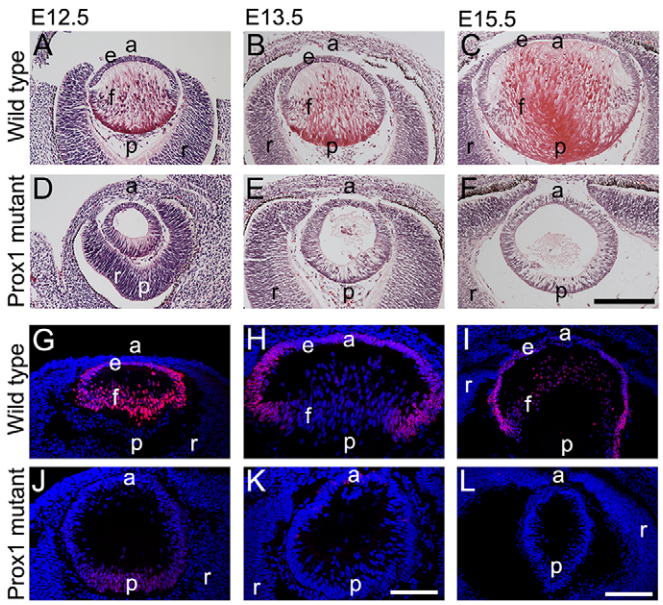

Fig. 1. *Prox1* deletion from the early lens arrests its development at the LV. (A-F) Mouse eye sections at E12.5 (A,D), E13.5 (B,E) and E15.5 (C,F) stained with Hematoxylin and Eosin. In WT, primary lens fibers (LFs; pink) were evident by E12.5 (A), with secondary fibers produced at E13.5 (B) and E15.5 (C). In *Prox1* cKO lenses, the posterior-most cells never elongate into eosinophilic primary (D) or secondary fibers (E,F). (G-L) Immunofluorescence staining for Prox1. Prox1 is expressed in WT primary LFs at E12.5 (G) and in elongating secondary LFs at E13.5 (H) and E15.5 (I). Prox1 protein levels are reduced in *Prox1* cKO by E12.5 (J), and Prox1 immunoreactivity is absent from *Prox1* cKO lenses by E13.5 (K,L). (A-F) Blue, Hematoxylin; pink, Eosin. (G-L) Blue, Draq5 (DNA); red, Prox1. a, anterior; p, posterior; r, retina; e, lens epithelium; f, LFs. Scale bars: 200 µm in A-F; 100 µm in G-L.

(Zhang et al., 1998). WT lenses express $p27^{Kip1}$ (not shown) and $p57^{Kip2}$ (Fig. 2C,C′) in differentiating LFs at E13.5, and a similar pattern was detected in the E13.5 *Prox1* cKO LV (not shown; Fig. 2D,D′).

WT E13.5 lenses exhibit little to no programmed cell death as measured by TUNEL (Fig. 2E,E′). *Prox1* cKO contained a few TUNEL-positive nuclei at E13.5 (Fig. 2F,F′). The vasculature surrounding WT lenses had few or no TUNEL-positive nuclei at E13.5 (Fig. 2E,E″), whereas *Prox1* cKO eyes exhibited apoptosis of the lens vasculature at E13.5 (Fig. 2F,F′), leading to its loss by E15.5 (Fig. 1F).

Prox1 cKO mice have reduced expression of LF cell markers

The morphological changes occurring during LF cell differentiation are coincident with a huge increase in crystallin expression (Duncan et al., 2004). Notably, mRNA levels of all crystallin genes assayed were significantly downregulated in *Prox1* cKO lenses compared with WT (Fig. 3A). Immunostaining using pan-specific β-crystallin (Fig. 3B) and γ-crystallin (Fig. 3C) antibodies revealed prominent LF-specific protein expression in WT lenses, whereas immunoreactivity was absent in *Prox1* cKO lenses (Fig. 3E,F). Further, the levels of aquaporin 0 (Mip – Mouse Genome Informatics), the most abundant LF membrane protein (Fig. 3D) (Bassnett et al., 2009), were reduced at the mRNA (Fig. 3A) and protein (Fig. 3G) levels in *Prox1* cKO compared with WT (Fig. 3D).

Prox1 cKO presumptive LFs appropriately decrease expression of lens epithelial markers

The expression of lens epithelial cell markers in the posterior LV is decreased as it initiates LF differentiation (Hawse et al., 2005).

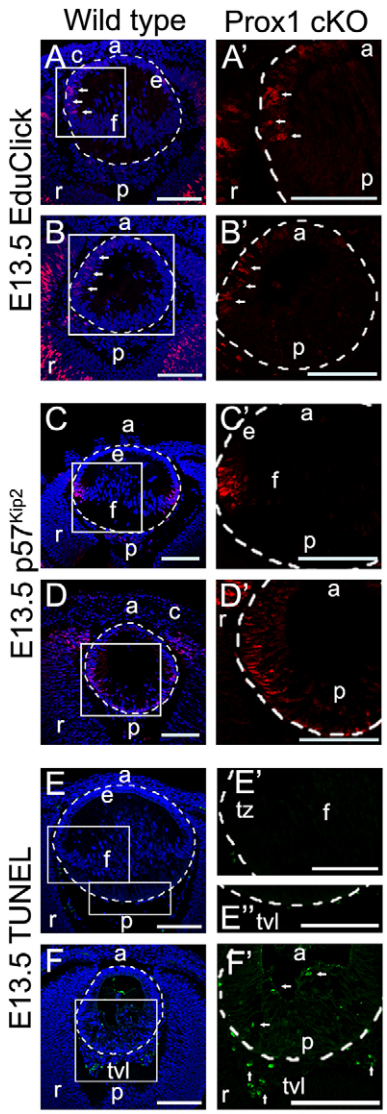

Fig. 2. Posterior cells of the *Prox1* cKO LV exit the cell cycle. (A,A′) E13.5 WT lenses exhibit EduClick (EduC)-positive cells (red) in the epithelium (arrows), but they were absent from the transition zone and from LFs. (B,B′) E13.5 *Prox1* cKO lenses maintained cell proliferation in the anterior aspect of the lens (arrows), while no EduC labeling was detected at the lens posterior. (C,C′) Immunofluorescence staining of WT E13.5 lenses showed expression of the cell cycle inhibitor $p57^{Kip2}$ (red) in differentiating LFs. (D,D′) Similarly, $p57^{Kip2}$ was still expressed in the most posterior cells of the *Prox1* cKO lens. (E-F′) TUNEL assays. Programmed cell death was not observed in WT lenses or the tunica vasculosa lentis at E13.5 (E,E′). Isolated TUNEL-positive nuclei were seen in the posterior LV of *Prox1* cKO at E13.5 (F,F′, arrows); however, robust TUNEL staining was consistently observed in the tunica vasculosa lentis of *Prox1* cKO at E13.5 (F,F′, arrows). Boxed regions in A-F are shown at higher magnification in A′-F′. The dashed line delineates the lens capsule. (A-F′) Blue, Draq5 (DNA). (A-B′) Red, EduC. (C-D′) Red, $p57^{Kip2}$. (E-F′) Green, TUNEL. a, anterior eye; p, posterior eye; r, retina; c, cornea; e, lens epithelium; tvl, tunica vasculosa lentis; f, LFs. Scale bars: 100 µm.

E-cadherin (cadherin 1) protein is restricted to the epithelium of E14.5 WT lenses (Fig. 4A), and this distribution is maintained in *Prox1* cKO lenses (Fig. 4B). The transcription factor Pax6 is abundant in the LV and lens epithelium (Fig. 4C), with lower levels present in LFs (Shaham et al., 2009). The highest Pax6 levels are restricted to the anterior cells of the *Prox1* cKO lens (Fig. 4D).

Development (2016) 143, 318-328 doi:10.1242/dev.127860

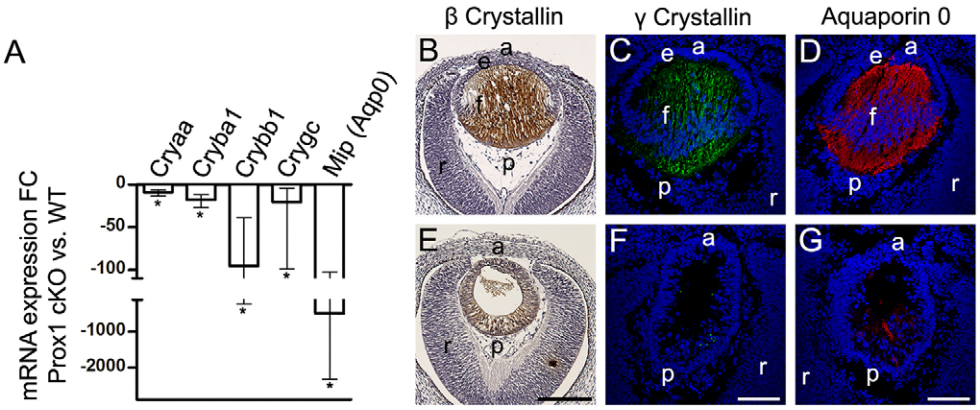

Fig. 3. LF marker expression decreases in *Prox1* cKO. (A) qRT-PCR of E14.5 *Prox1* cKO lenses compared with WT. *$P \leq 0.01$ by nested ANOVA. αA-crystallin (*Cryaa*; $P=0.007$), βA1-crystallin (*Cryba1*; $P=0.001$), βB1-crystallin (*Crybb1*; $P=0.002$), γC-crystallin (*Crygc*; $P=0.0001$) and aquaporin 0 ($P=0.004$) mRNA levels are reduced in *Prox1* cKO lenses. Error bars indicate s.d.; $n=3$. (B,E) β-crystallin protein (brown) localizes to WT LFs at E13.5 (B), but this is reduced in *Prox1* cKO lenses (E). (C,F) γ-Crystallin protein (green) is found in elongated LFs in the E13.5 WT lens (C), but its levels are reduced in the *Prox1* cKO lens (F). (D,G) Aquaporin 0 protein (red) is found in E13.5 WT LFs (D), whereas little is detected in *Prox1* cKO lenses (G). (B,E) Blue, Hematoxylin. (C,D,F,G) Blue, Draq5 (DNA). a, anterior eye; p, posterior eye; r, retina; e, lens epithelium; f, LFs. Scale bars: 200 µm in B,E; 100 µm in C,D,F,G.

Global gene expression profiling reveals that Prox1 is a major regulator of lens-enriched gene expression

RNA-seq was performed on E13.5 lenses to elucidate how the lens transcriptome is affected immediately following the loss of Prox1 protein expression (full data are available at GEO under accession GSE69940). Overall, 642 genes were differentially expressed in the E13.5 *Prox1* cKO lens; 356 were expressed at lower levels in *Prox1* cKO lenses [referred to as downregulated differentially expressed genes (downDEGs); Table S3], whereas 286 were elevated in *Prox1* cKO [upregulated differentially expressed genes (upDEGs); Table S4].

Analysis of downDEGs using DAVID (Huang et al., 2009) (Fig. 5A) revealed that the most significant gene ontology (GO) category was 'structural constituents of the eye lens', which included every crystallin known to be an LF cell marker in embryos (*Cryaa*, *Cryba1*, *Cryba2*, *Cryba4*, *Crybb1*, *Crybb3* and all gamma crystallins) as well as aquaporin 0. *Prox1* cKO downDEGs were also enriched in regulators of cytoskeletal organization as well as the LF-enriched, RNA granule-encoding genes *Tdrd7* (Lachke et al., 2011) and *Caprin2* (Dash et al., 2015). Notably absent were genes that regulate the cell cycle, consistent with our findings presented in Fig. 2.

The most enriched GO category of upDEGs (Fig. 5B) included genes involved in cell adhesion. Others included genes associated with non-LF cell lineages such as skeletal system development and melanin biosynthesis. Taken together, these data indicate that Prox1 turns off the expression of genes associated with non-lens lineages, while positively regulating the expression of effectors of LF morphogenesis and function.

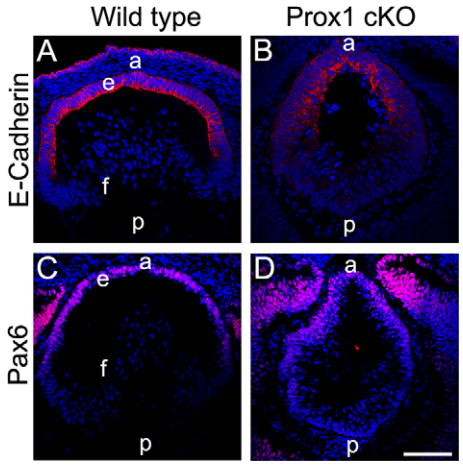

Fig. 4. *Prox1* cKO lenses have a normal distribution of epithelial markers. (A,B) E-cadherin (red) is expressed in the epithelium and absent at the transition zone of both WT (A) and *Prox1* cKO (B) E13.5 lenses. (C,D) The transcription factor Pax6 (red) is preferentially localized to the lens epithelium and reduced at the transition zones of both WT (C) and *Prox1* cKO (D) lenses at E14.5. Blue, Draq5 (DNA). a, anterior eye; p, posterior eye; e, lens epithelium; f, LFs. Scale bar: 100 µm.

A majority of genes downregulated in the *Prox1* cKO exhibit lens-enriched expression

DAVID categorizes differentially expressed genes (DEGs) into functionally related groups. However, it does not address the expression dynamics of DEGs in normal lens development – information that can provide additional insights into the significance of Prox1 in lens biology. Therefore, the effect of Prox1 on the expression of genes crucial for lens phenotype was determined by examining which DEGs are preferentially expressed in the lens using *iSyTE*, a tool that identifies genes with lens-enriched expression by ranking them based on a 'lens-enrichment score'. The lens-enrichment score for a gene is defined as the measure of its fold difference in expression between the lens and the whole embryonic body reference at $P<0.05$. Lens-enrichment scores change as lens differentiation proceeds from the lens pit at E10.5 to the early lens at E12.5, potentially indicating that a gene exhibits enriched expression in differentiating LFs (Lachke et al., 2012). Fig. 5C-H plots the fold change (FC) in expression between DEGs in *Prox1* cKO lenses against their *iSyTE* lens-enrichment scores. From the onset of LF differentiation at E12.5 through postnatal stages, most downDEGs were lens enriched; note the clustering of the *Prox1* cKO downDEGs in the upper left quadrant of Fig. 5E-H. By contrast, most upDEGs were not lens enriched, and this trend became more obvious following the onset of LF differentiation (see lower right quadrant of Fig. 5E-H). The lens-enrichment scores of the downDEGs were significantly higher than those of the upDEGs at all stages examined. However, this relationship was especially obvious after the onset of LF differentiation (E12.5) (Fig. 5E-H).

Further, comparison of the genes that *iSyTE* identified as 'most lens enriched' with the DEGs in *Prox1* cKO lenses demonstrated

Development (2016) 143, 318-328 doi:10.1242/dev.127860

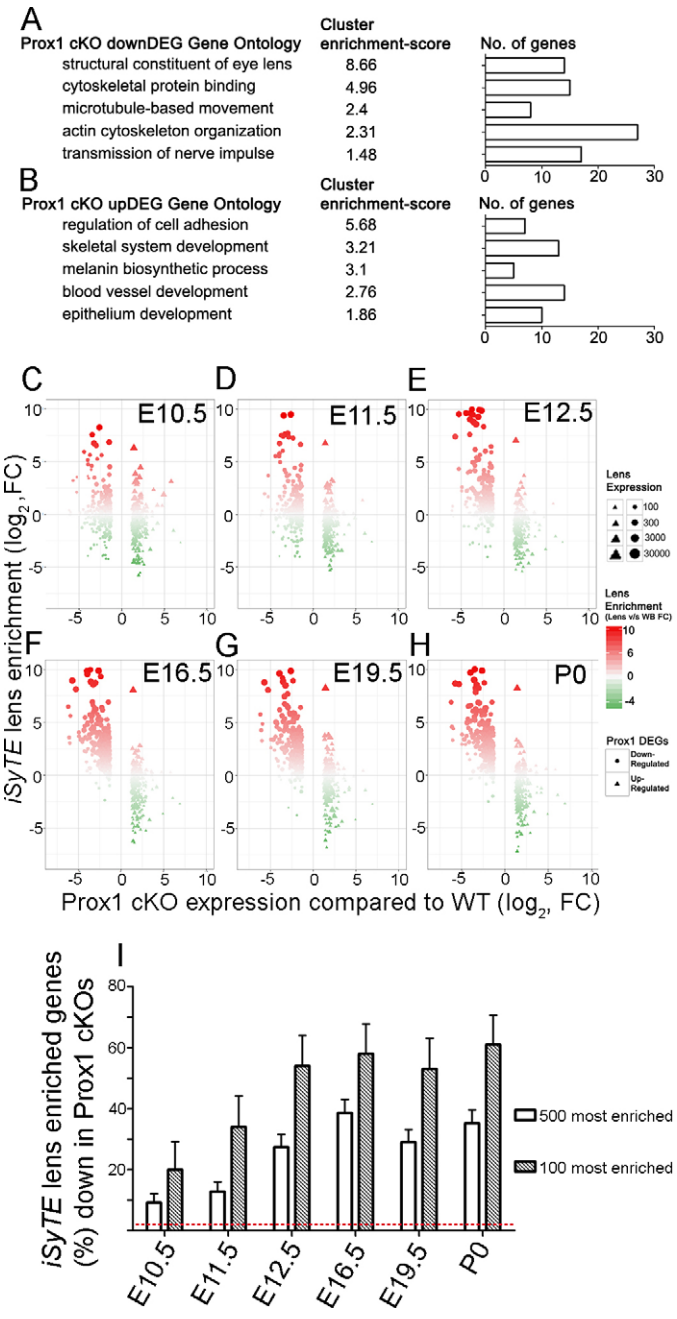

Fig. 5. *Prox1* deletion results in the misregulation of genes that are highly enriched in expression in the developing lens. RNA-seq was performed on E13.5 *Prox1* cKO and WT lenses immediately following the loss of Prox1 protein. (A,B) The DAVID bioinformatics resource was used to group/cluster the downregulated (downDEGs) (A) and upregulated (upDEGs) (B) genes into functionally related gene ontology (GOs) categories with cluster enrichment scores representing their likelihood of affecting biological function. (C-H) The relative lens-enrichment score of each DEG [FC, fold change from the whole body (WB) control] at E10.5 (C), E11.5 (D), E12.5 (E), E16.5 (F), E19.5 (G) and P0 (H) was determined using *iSyTE*. The values obtained were plotted in a dot plot with *Prox1* cKO DEGs [fold change (FC) of gene expression in *Prox1* cKO lens compared with WT control] on the *x*-axis. The *iSyTE* lens enrichment in expressed as FC compared with the WB reference dataset (as described by Lachke et al., 2012) on the *y*-axis. As shown in the key, the size of the solid circles (downregulated in *Prox1* cKO) or triangles (upregulated in *Prox1* cKO) represents the lens expression levels in microarray fluorescence intensity units (data obtained from *iSyTE* and other publically available datasets). The color of the circles or triangles represents lens-enrichment scores in FC (red, lens-enriched genes; green, genes expressed at higher levels in the WB reference). As the lens progresses from E12.5 to P0, the vast majority of DEGs in the downDEGs category fall into the lens-enriched (upper left quadrant) category compared with upDEGs (upper right quadrant), which was significant by a χ^2 test for goodness of fit (P<0.00001). Notably, χ^2 values increased between the LV and the onset of LF differentiation (see Materials and Methods). (I) The fraction of the top 500 or top 100 lens-enriched genes at various developmental stages that are downregulated in *Prox1* cKO. Error bars indicate s.e.m.; n=3. Red dotted line indicates the percentage of genes expected to be downregulated in a random sample.

that Prox1 is required for the expression of a significant, although relatively small, fraction of lens-enriched genes at E10.5 (LV). However, as LF differentiation begins at E12.5, the requirement for Prox1 in regulating the lens developmental program increases dramatically (Fig. 5I). Prox1 was required for the expression of 54% of the top 100 most lens-enriched genes at E12.5, a figure that increased to 60% during secondary LF differentiation (Fig. 5I). A χ^2 test for goodness of fit found this to differ significantly from random chance (P<0.0001, two-tailed t-test).

These data support the idea that Prox1 plays major roles in regulating the gene expression that confers the LF cell phenotype.

FGFR expression decreases in *Prox1* mutants

As none of the *Prox1* cKO DEGs included known transcriptional regulators of LF cell differentiation (Tables S3 and S4), *Prox1* cKO DEGs were searched for genes involved in regulatory loops known to control LF fate. FGF regulates LF differentiation by binding to transmembrane FGF receptors (FGFRs) on lens cells (Lovicu and McAvoy, 2005), and the simultaneous removal of *Fgfr1*, *Fgfr2* and *Fgfr3* results in a failure of LF differentiation similar to the *Prox1* cKO phenotype (Zhao et al., 2008). Notably, *Fgfr3* mRNA levels decreased 10-fold in the lens following Prox1 loss, whereas *Fgfr1* and *Fgfr2* were unchanged (Table 1). This was validated in E14.5 WT and *Prox1* cKO lenses by qRT-PCR (Fig. 6A).

Interestingly, RNA-seq identified two additional genes that could regulate FGF signaling in the lens. FGF receptor-like 1 (*Fgfrl1* or *Fgfr5*) is the most abundant FGFR mRNA in the E13.5 lens, and its levels are 4-fold reduced in *Prox1* cKO lenses (Table 1). Lactase-like (*Lctl*, klotho γ or *Klph*) was the most profoundly downregulated

Table 1. FGF receptor and co-receptor mRNA levels in *Prox1* cKO versus WT lenses determined by RNA-seq

FGFR and FGF co-receptor expression from *Prox1* cKO versus WT RNA-seq

Gene symbol	Gene description	WT RPKM	FC
FGFR gene expression			
Fgfr1	Fibroblast growth factor receptor 1	15	−1.14
Fgfr2	Fibroblast growth factor receptor 2	13.4	−1.23
Fgfr3	Fibroblast growth factor receptor 3	23.9	−10.8
Fgfr4	Fibroblast growth factor receptor 4	0.095	1
Fgfrl1 (*Fgfr5*)	Fibroblast growth factor receptor-like 1	32.3	−4.2
Klotho gene expression			
Lctl	Lactase-like (klotho gamma)	2.34	−234
Kl	Klotho	0.002	1
Klb	Klotho beta	0.051	1

The mean transcript abundance for each FGFR is given in reads per million per kilobase (RPKM). Differential gene expression between WT and *Prox1* cKO lenses is represented by fold change (FC).

Development (2016) 143, 318-328 doi:10.1242/dev.127860

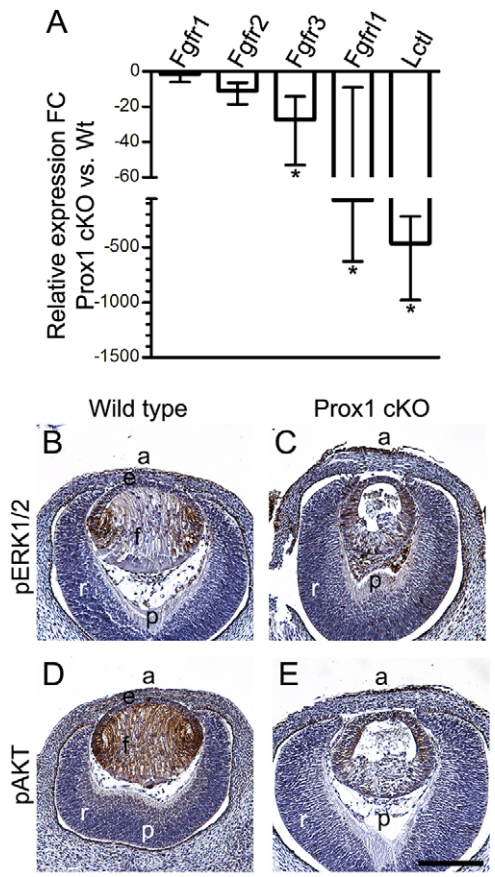

Fig. 6. *Prox1* cKO lenses exhibit a decrease in the expression of three FGFRs and their downstream signaling. (A) qRT-PCR revealed significant decreases in the expression of *Fgfr3* (P=0.01), the atypical receptor *Fgfrl1* (P=0.04), and the FGF co-receptor *Lctl* (P=0.03) in E14.5 *Prox1* cKO lenses; *P<0.05 by nested ANOVA. Error bars indicate s.d.; n=3. (B) By immunohistochemistry pErk1/2 (brown) was detected at the transition zones of WT lenses (B) and was absent from the equator of *Prox1* cKO lenses (C) at E13.5. Similarly, robust pAKT staining (brown) was observed at the transition zones of WT lenses at E13.5 (D), but was absent in the posterior LFs of *Prox1* cKO lenses (E). Blue, Hematoxylin. a, anterior; p, posterior, r, retina; e, epithelium; f, LFs. Scale bar: 100 µm.

gene following Prox1 loss and is the only Klotho family member expressed in the lens (Table 1). The downregulation of these genes was confirmed and found to be even more profound at E14.5 by qRT-PCR (Fig. 6A).

Prox1 cKO lenses exhibit reduced MAPK and AKT activation

Since *Prox1* deletion led to significant reductions in FGFR mRNA levels in the lens, we next determined if these changes resulted in decreased FGFR-mediated signal transduction. Ligand association with FGFRs initiates signaling through MAPK and PI3K/AKT pathways to stimulate LF differentiation (Wang et al., 2009). Phosphorylated (p) Erk1/2 (Mapk3/1; MAPK effector) was found at the WT transition zone (Fig. 6B), whereas *Prox1* cKO lenses exhibited less active Erk1/2 at the lens equator, although apparently normal levels of the pErk1/2 were observed in the lens epithelium (Fig. 6C). pAKT is detected in the differentiating LFs of E14.5 WT lenses (Fig. 6D). By contrast, AKT phosphorylation was decreased in the presumptive LFs of *Prox1* cKO mice (Fig. 6E), although pAKT levels appeared unaffected in the anterior-most lens cells. These data suggest that decreased FGFR expression in *Prox1* cKO lenses decreases FGFR-mediated signal transduction.

Putative Prox1 binding sites in *Fgfr3*, *Fgfrl1* and *Lctl* are evolutionarily conserved and Prox1 binds to these genes in the lens *in vivo*

Since FGFR expression and signaling are attenuated in the *Prox1* cKO lens, the potential for Prox1 to directly bind to the FGFR promoters was assessed. The regions upstream of the transcriptional start site (TSS) of the human, mouse and chicken *Fgfr3*, *Lctl* and *Fgfrl1* genes were searched for the three previously described Prox1 binding motifs (Chen et al., 2008). These genes were then aligned, revealing that several predicted Prox1 binding sites are evolutionarily conserved in the putative *Fgfr3* (Fig. 7A), *Fgfrl1* (Fig. 7B), *Lctl* (Fig. 7C) promoters. Chromatin immunoprecipitation (ChIP) was performed on chicken embryonic lenses and revealed that Prox1 is likely to bind upstream of the TSS of all three genes, as measured by statistically significant enrichment of fragment recoveries compared with a region 5 kb downstream of the putative TSS (Fig. 7D-F). One caveat to this conclusion is that the chicken *LCTL* gene annotation was only provisional. These data are consistent with the prior identification of evolutionarily conserved Prox1 binding sites in the *FGFR3* promoter, and the ability of Prox1 to bind to these sites in electrophoretic mobility shift assays (Shin et al., 2006).

Prox1 expression is regulated by FGFR signaling

Prox1 protein levels increase sharply coincident with LF differentiation (Fig. 1I-K) (Duncan et al., 2002), and mice lacking Fgfr1-3 from the lens downregulate Prox1 protein levels (Zhao et al., 2008), suggesting that FGF signaling regulates Prox1 levels in the lens. Rat lens epithelial explants were cultured in a high dose of FGF, which promotes LF-like differentiation and morphology (McAvoy and Chamberlain, 1989). Although the explants cultured without FGF survived (Fig. 8A-C), only explants cultured with a differentiating dose of FGF (Fig. 8D-F) exhibited robust Prox1 expression (Fig. 8F). Further, when explants were cultured with a high dose of FGF and either an antagonist of FGFR signaling (Fig. 8G-I) or an inhibitor of the MAPK pathway effector Mek1 (Map2k1) (Fig. 8J-L), nuclear Prox1 levels were attenuated (Fig. 8I,L). Western blot analysis confirmed the upregulation of Prox1 expression in rat lens explants in response to FGF and the attenuation of this response by a MAPK inhibitor (Fig. 8M,N). Notably, inhibition of PI3K/AKT signaling did not affect Prox1 upregulation in response to FGF (Fig. 8M,N). These data suggest that the dramatic increase in Prox1 protein at the onset of LF differentiation is regulated by FGF signaling through FGFRs in a largely MAPK-mediated pathway.

DISCUSSION

Prior to this work, Prox1 function in lens development was understudied. Prox1 expression was known to correlate with LF differentiation (Duncan et al., 2002) and to be required for LF morphogenesis (Wigle et al., 1999), but, whereas *in vitro* experiments suggested that Prox1 regulates the expression of LF differentiation markers (Chen et al., 2008; Lengler et al., 2001), this was not supported by the only *in vivo* investigation performed on Prox1 function in lens (Wigle et al., 1999). In the present study we sought to expand our understanding of the mechanisms by which Prox1 mediates LF differentiation.

Prox1 is not a major regulator of cell cycle exit after LV closure

Prior work on *Prox1* null mice demonstrated that the lens is arrested at the LV stage, indicating an essential role of Prox1 in LF cell morphogenesis. It was proposed that Prox1 generates LV

Development (2016) 143, 318-328 doi:10.1242/dev.127860

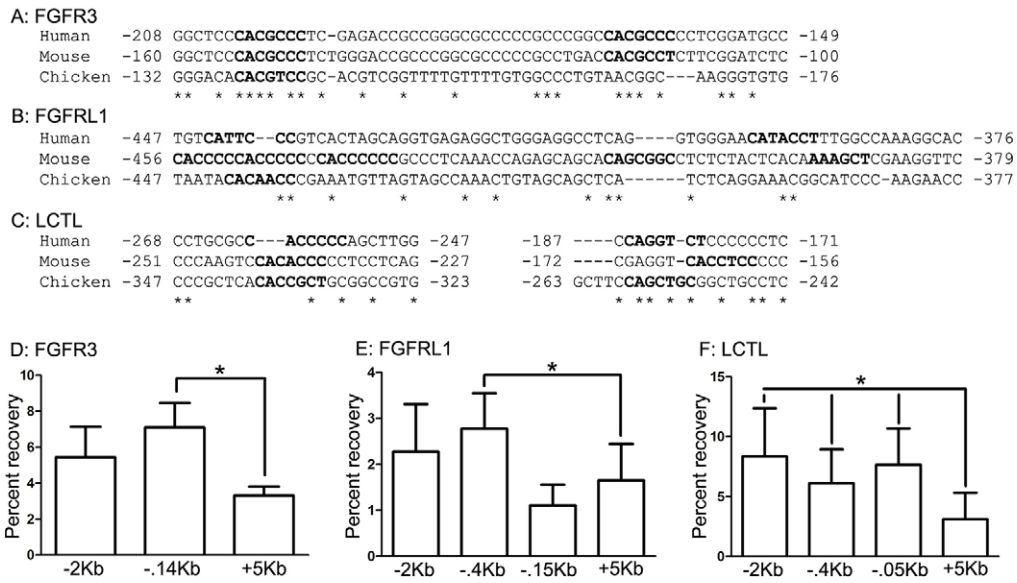

Fig. 7. Prox1 binds to the putative *FGFR3*, *FGFRL1* and *LCTL* promoters as assayed by ChIP. (A-C) The regions upstream of the transcriptional start site (TSS) of *Fgfr3*, *Fgfrl1* and *Lctl* were screened for matches to the Prox1 consensus binding sequences: (A or C) AAG(N)(not A) or CA(not A)(N)(N)(C or G)(C or T) (Chen et al., 2008). Putative Prox1 binding sites (bold) were identified in the *Fgfr3* promoters of human, mouse and chicken (A), which matched the previously characterized Prox1 binding sites in the human *FGFR3* promoter (Shin et al., 2006) and are numbered relative to the TSS. Predicted Prox1 binding sites (bold) are present upstream of human, mouse and chicken *Fgfrl1* (B) and *Lctl* (C) putative TSSs. (D-F) ChIP was performed on embryonic chicken lenses, pulling down chromatin complexed with Prox1 protein. DNA fragments corresponding to the regions upstream of *FGFR3* (D), *FGFRL1* (E) and *LCTL* (F) were recovered at an enriched frequency when compared with regions 5 kb downstream of each TSS, as assayed by qRT-PCR followed by two-way ANOVA with $*P \leq 0.05$. Error bars indicate s.d.; $n=3$.

polarity by downregulating the expression of E-cadherin in the posterior LV and upregulating expression of the cell cycle inhibitors $p27^{Kip1}$ and $p57^{Kip2}$ (Wigle et al., 1999). By contrast, although *Prox1* cKO lenses in the present study exhibited morphological similarities to *Prox1* null lenses, they differed at the molecular level. In *Prox1* cKO lenses, E-cadherin was restricted to the anterior LV (Fig. 4B), while $p27^{Kip1}$ and $p57^{Kip2}$ expression was maintained posterior to the lens equator (not shown; Fig. 2D,D′). This difference in phenotype is likely to be derived from the timing of Prox1 loss, as the *Prox1* cKO lenses do not lose all Prox1 protein until after LV closure (Fig. 1K), whereas Prox1 was absent from all tissues in the prior report (Wigle et al., 1999). The observation that a lack of cell cycle exit is insufficient to explain the *Prox1* null lens phenotype is consistent with prior reports of retinoblastoma mutant (Fromm et al., 1994; Pan and Griep, 1994) and $p27^{Kip1-/-};p57^{Kip2+/-}$ (Zhang et al., 1998) lenses, which do not phenocopy the morphology of lenses lacking Prox1, despite maintaining cell proliferation in the posterior lens.

Prox1 is a major regulator of LF cell-enriched gene expression

Prox1 cKO lenses exhibited decreased levels of every LF marker that was assayed by immunolocalization and qRT-PCR (Fig. 3). Then, RNA-seq was performed on *Prox1* cKO lenses as an unbiased approach to discover potential pathways regulated by Prox1 in the lens. DAVID-based analysis of DEGs showed that many downDEGs have a known function in the lens. On the other hand, *iSyTE* allowed an appreciation of the dynamic expression of all DEGs in normal lens development. Specifically, the analysis of *Prox1* cKO DEGs by *iSyTE* suggests that *Prox1* cKO downDEGs are normally upregulated in expression during LF differentiation. Further, these data suggest that Prox1 is required for the expression of 60% of genes exhibiting the most highly lens-enriched expression pattern at these developmental time points (Fig. 5).

Although these findings contrast with a prior report that suggested that Prox1 had no significant role in lens marker expression, this is likely to be due to the non-quantitative nature of that study (Wigle et al., 1999). Notably, prior ChIP analyses show that the βB1-crystallin locus (downregulated 7-fold in E13.5 *Prox1* cKO lens as assessed by RNA-seq; 95-fold in E14.5 *Prox1* cKO lens as assessed by qRT-PCR, see Fig. 3) is bound by Prox1 in lens chromatin (Chen et al., 2008), while co-transfection analyses show that both the βB1-crystallin (Chen et al., 2008; Cui et al., 2004) and γF-crystallin (downregulated 44-fold in the E13.5 *Prox1* cKO lens) (Lengler et al., 2001) promoters have functional Prox1 binding sites. Together, these data support the idea that Prox1 directly regulates at least a subset of genes that express markers of LF cell differentiation.

Prox1 cKO downDEGs may shed light on the molecular mechanisms underlying LF morphogenesis

Differentiating LFs undergo massive morphological changes, which include cytoskeleton rearrangements that are required for LF elongation. DAVID analysis of the *Prox1* cKO DEGs suggested that Prox1 regulates this process. As lens epithelial cells differentiate into LF cells, they dismantle actin stress fibers in response to PI3K/AKT signaling (Weber and Menko, 2006b) and repolymerize them into cortical actin bundles that reside under the LF cell plasma membrane (Weber and Menko, 2006a). Notably, the *Prox1* cKO downDEGs include numerous genes that could regulate actin (Fig. 5A) and therefore might be involved in this process. The ultimate lack of LF cell elongation could result from both the loss of fiber cell-enriched actin regulators and the attenuation of AKT signaling (Fig. 6E) observed in *Prox1* cKO lenses.

Elongating LFs also require microtubules, as the culture of lens cells in inhibitors of microtubule polymerization or monomer association significantly decreases LF elongation (Piatigorsky, 1975). The *Prox1* cKO downDEGs include several genes that may regulate microtubule dynamics, including tubulin itself, as well

Development (2016) 143, 318-328 doi:10.1242/dev.127860

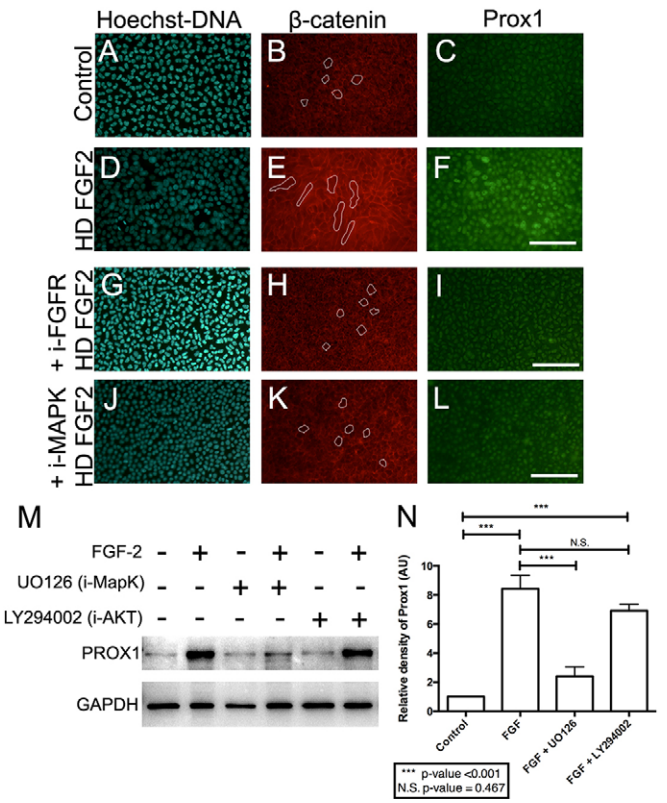

Fig. 8. Prox1 expression is regulated by FGFR-mediated MAPK signaling. (A-C) Explants cultured without FGF2 maintained their cuboidal epithelial morphology (B, cell outlines) and did not upregulate Prox1 (C). (D-F) Explants cultured in a high dose (100 ng/ml) of FGF2 displayed cell multi-layering and cell elongation (E, cell outlines), features of LF differentiation *in vitro*, and exhibited elevated levels of nuclear Prox1 (F). (G-I) When cultured in the presence of the FGFR antagonist SU5402, explants maintained their cuboidal epithelial morphology (H, cell outlines) and did not increase their nuclear Prox1 expression (I) in response to FGF2, similar to controls not treated with FGF2 (C). (J-L) When cultured in the presence of an inhibitor of the MAPK pathway kinase Mek1 (UO126), explants maintained their cuboidal epithelial morphology (K, cell outlines) and slightly increased their nuclear Prox1 expression (L) in response to FGF2, as compared with controls not treated with FGF2 (C); however, these explants did not recapitulate the upregulation of nuclear Prox1 observed in non-inhibited samples (F). (M,N) Explants cultured with or without (100 ng/ml) FGF2 and with or without inhibitors were analyzed by western blot for Prox1 and Gapdh. Blots were quantified by densitometry using ANOVA followed by a Šídák multiple comparison post-test and are presented with s.e.m. Induction of LF differentiation with FGF2 resulted in a significant upregulation of Prox1 that was blocked by addition of the MAPK inhibitor UO126 but not significantly blocked by addition of the PI3K/AKT inhibitor LY294002. Blue, Hoechst; red, β-catenin; green, Prox1. Scale bars: 100 µm.

as other tubulin-interacting proteins. Further, the downDEGs include regulators of transport along microtubule bundles, which may traffic materials required for LF elongation. Overall, these data suggest that Prox1 plays a major role in modulating the cytoskeletal dynamics in the lens that is required for LF elongation.

Prox1 regulates the expression of Fgfr3, Lctl and Fgfrl1

This study suggests that, similar to its role in the lymphatic vasculature (Johnson et al., 2008), Prox1 regulates the expression of Fgfr3 in the lens. However, as a single copy of any of the *Fgfr1-3* genes is sufficient to rescue the LF-deficient phenotype in FGFR triple-null mice (Zhao et al., 2008), the downregulation of Fgfr3 alone in *Prox1* cKO lenses does not explain the profound reduction in pERK and pAKT levels observed. Notably though, two other transmembrane FGF-interacting proteins, Lctl and Fgfrl1, might contribute to this phenotype.

Lctl is a transmembrane FGF-binding protein of the Klotho family (Fon Tacer et al., 2010). Signaling through canonical FGFRs requires their association with both FGFs and heparan sulfate (HS) (Schlessinger et al., 2000). Whereas canonical FGFs interact readily with both HS and FGFRs, the FGF19 subfamily has low affinity for HS (Goetz et al., 2007). Thus, FGF19 subfamily members are not sequestered by HS-containing extracellular matrix and can travel further from their origin to act in an endocrine fashion. Their target cells are sensitized to this endocrine signal by expression of Klotho transmembrane receptors, such as Lctl, which bind to FGF19 family members and FGFRs to stabilize the FGF19-HS-FGFR complex, allowing for signal transduction (Goetz et al., 2007; Kurosu et al., 2007). *Lctl* is the only Klotho expressed in the lens (Table 1), and it is the most downregulated gene following Prox1 loss (Table S3), suggesting that it is nearly absent in lenses that do not express Prox1. Lctl would be expected to associate with Fgfr1 and 2 in the lens to facilitate their interaction with Fgf15/19 (Fon Tacer et al., 2010), and thus a loss of Lctl is expected to dramatically decrease the response of Fgfr1 and 2 to endocrine FGFs. Further, we demonstrate that Prox1 binds to the putative *LCTL* promoter in the chicken lens *in vivo*. Therefore, we propose that the onset of Prox1 expression at the lens transition zone might upregulate Lctl levels to sensitize presumptive LFs to FGF19 family members, whereas neighboring epithelial cells, which lack strong nuclear Prox1 expression, would have much lower levels of Lctl and thus not respond to FGF19 protein.

The expression of Fgfrl1, a transmembrane FGFR that lacks an intracellular kinase domain (Steinberg et al., 2010), is downregulated in *Prox1* cKO lenses (Figs 6 and 7). Fgfrl1 was presumed to inhibit FGF signaling by sequestering ligand (Steinberg et al., 2010). However, new evidence suggests that Fgfrl1 facilitates FGF ligand-dependent MAPK activation (Silva et al., 2013). Further, Fgfrl1 also enhanced FGF-stimulated Erk1/2 activation, implicating a role in ligand-dependent signaling (Silva et al., 2013). Intriguingly, Fgfrl1 also increases basal Erk1/2 phosphorylation independently of FGF ligand. Since Fgfrl1 expression is downregulated in *Prox1* cKO lenses, Prox1 expression in the posterior LV is likely to increase Fgfrl1 expression to augment MAPK signal transduction.

Overall, downregulation of these receptors in *Prox1* cKO decreases the FGF signaling capacity of the lens, as Fgfr3 is the most highly expressed of the canonical FGFRs in the lens (Table 1) and interacts with a wide array of paracrine FGF ligands (Robinson, 2006). Fgfrl1 is expressed at even higher levels than Fgfr3 in the lens, and Lctl is required for signaling in response to endocrine Fgf15/19, which is required for lens and retina development in zebrafish and chicken (Kurose et al., 2005; Nakayama et al., 2008). The ChIP experiments suggest that the *Fgfr3*, *Fgfrl1* and *Lctl* promoters are regulated by Prox1; however, further experiments are necessary to definitively show whether the effect of Prox1 on the expression of these FGFRs is direct or indirect.

Prox1 and FGFRs form a novel regulatory loop that regulates the differentiation of lens epithelial cells into LFs

Previous studies have shown that FGF is sufficient to trigger lens epithelial cell differentiation into LFs (Lovicu and McAvoy, 2005). Correspondingly, FGFRs are present at low levels in lens epithelia and the LV, whereas their expression increases dramatically proximal to the onset of LF elongation (de Iongh et al., 1997). If FGFR expression does not reach sufficient levels, LVs are unable to

Development (2016) 143, 318-328 doi:10.1242/dev.127860

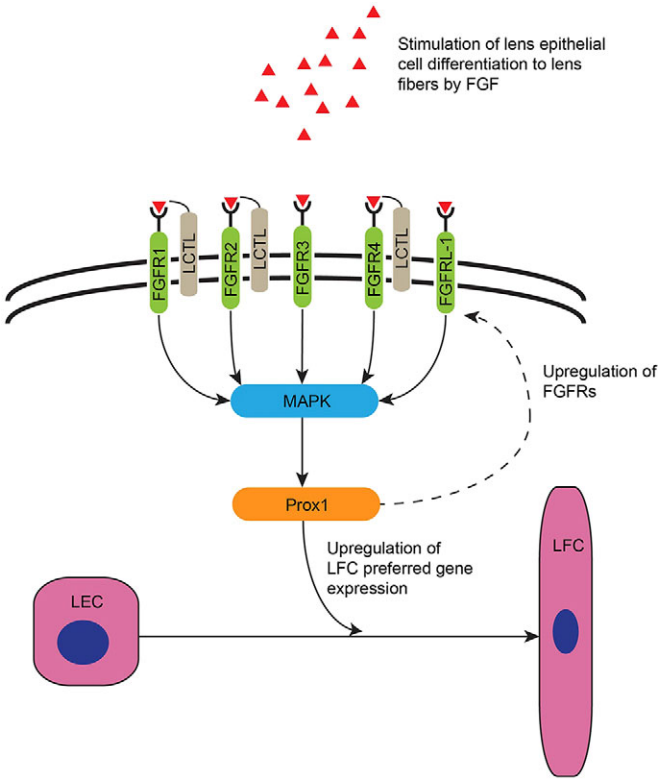

Fig. 9. Model of Prox1 crosstalk with FGFRs. In normal lenses, FGFs interact with the canonical FGFR1-4, or with FGFRL1, to drive intracellular signaling. LCTL facilitates the interaction of FGFR1,2,4 with endocrine FGFs. Activation of FGFRs promotes signaling via the MAPK pathway, upregulating Prox1 expression in response to FGF stimulation. Further, Prox1 upregulates *Fgfr3*, *Fgfrl1* and *Lctl* expression through direct promoter interactions, sensitizing these cells to respond to FGFs, driving LF differentiation. LEC, lens epithelial cell; LFC, lens fiber cell.

respond to FGF, resulting in failure of LF differentiation (Zhao et al., 2008). However, the mechanism by which lens epithelial cells upregulate FGFR expression was previously unclear. Prox1 protein levels are dramatically upregulated in the posterior LV and at the onset of secondary fiber differentiation throughout life (Duncan et al., 2002), a process that is dependent on FGFR signaling in the lens (Li et al., 2014; Zhao et al., 2008). Here, we demonstrate that exogenous FGF is sufficient to stimulate nuclear Prox1 levels in lens explants and that this process requires signaling through the MAPK pathway (see Fig. 8). Thus, we propose that signaling through FGFRs in response to endogenous FGF causes differentiating LFs to increase Prox1 levels. Prox1 may then feedback to transcriptionally upregulate FGFR expression, initiating a positive-feedback loop that rapidly increases FGFR and Prox1 levels. These data implicate Prox1 in this process, but it is possible that Prox1 acts in coordination with as yet unidentified factors (Fig. 9).

In summary, these findings suggest that Prox1 participates in a positive-feedback loop with FGFRs to sensitize differentiating LFs to the surrounding FGF ligand. This process, in turn, is responsible for the regulation of a large proportion of the genes required for LF differentiation.

MATERIALS AND METHODS

Animals

Mice harboring a conditional *Prox1* allele in which exons 3 and 4 (encoding the homeo-prospero domain) are flanked by LoxP sites (Prox1tm2Gco) (Harvey et al., 2005), were obtained from Dr Guillermo Oliver (St Jude Children's Research Hospital, Memphis, TN, USA). These mice were crossed with MLR10Cre mice expressing Cre recombinase throughout the lens beginning at the LV (Zhao et al., 2004), which were obtained from Dr Michael Robinson (Miami University, Oxford, OH, USA) and backcrossed with C57BL/6<Har> for at least four generations. C57BL/6<Har> mice were used as WT controls. E0.5 represents noon of the day the vaginal plug was observed. Mice were genotyped for the *Prox1* flox allele and *MLR10Cre* as described in Table S1. Histology was performed as described previously (Manthey et al., 2014a). No lens defects were observed in mice homozygous or heterozygous for either the *MLR10Cre* transgene or the *Prox1* flox allele alone.

Immunofluorescence

Most immunofluorescence was performed as reported previously (Reed et al., 2001), except that Draq5 (1:2000; Biostatus) was used as the nuclear counterstain and imaging was performed on a Zeiss LSM780 confocal microscope. Specific staining protocols are provided in Table S2. $p57^{Kip2}$ (Santa Cruz, sc8298; 1:100) immunostaining was performed on paraffin sections subjected to antigen retrieval by boiling in 0.01 M sodium citrate buffer pH 6.0, and treatment with 1% Saponin (Sigma-Aldrich). Expression patterns were compared using slides stained simultaneously and scanned using identical imaging settings. Some images were processed to increase brightness or contrast using Photoshop (Adobe Systems); however, all adjustments were applied equally to all images within an experimental/control group.

Immunohistochemistry

Immunohistochemical staining for β-crystallin was performed as described previously (Firtina et al., 2009). Immunohistochemical staining for pErk1/2 (Cell Signaling, cs4377s; 1:50) and pAKT (Cell Signaling, cs9271s; 1:50) was performed on antigen-retrieved paraffin sections using the CSAII Biotin-Free Tyramide Signal Amplification Kit with the CSA II Rabbit Link (Dako, Agilent).

Cell proliferation assays

Cells in S phase were detected using 5-ethynyl-2′-deoxyuridine (EdU) Click-iT cell proliferation assays (Invitrogen). Pregnant mice were injected intraperitoneally with 800 µg EdU. Three hours later, embryos were collected, sectioned, and the Click-it reactions performed as previously described (Mamuya et al., 2014).

TUNEL assay

DNA fragmentation was detected by terminal deoxynucleotidyl transferase dUTP nick end labeling (TUNEL) using the In Situ Cell Death Detection Kit, Fluorescein (Roche). Paraffin sections were subjected to antigen retrieval and TUNEL performed following the manufacturer's directions.

RNA isolation and quantitative real-time PCR (qRT-PCR)

RNA was isolated from lenses collected by the microdissection of E14.5 *Prox1* cKO and WT mice (20 lenses per biological replicate) using the SV Total RNA Kit (Promega). cDNA was synthesized using the SABiosciences RT2 First Strand Kit (Qiagen). qRT-PCR was carried out using QuantiTect SYBR Green (Qiagen) on an ABI7300 Real-Time PCR system (Applied Biosystems) and mRNA levels for each gene were normalized to the 18S ribosomal subunit (Mamuya et al., 2014). Differential expression was determined using the ΔΔCT method (Bookout and Mangelsdorf, 2003) and significance determined by nested ANOVA. The primer sets used for qRT-PCR are listed in Table S1.

RNA-seq

The RNA-seq methods were recently published (Manthey et al., 2014a,b), so only deviations are noted. Embryonic lenses were collected from E13.5 *Prox1* cKO and WT mice by microdissection (30 lenses/sample, three biological replicates/genotype) and total RNA isolated. cDNA libraries were constructed using the Illumina TruSeq RNA Sample Preparation Kit v2, and sequenced using an Illumina HiSeq 2000 (University of Delaware

Development (2016) 143, 318-328 doi:10.1242/dev.127860

Sequencing Center). Reads were processed using the CLC Genomics server, and mapped to the *Mus musculus* GRCm38.77 genome build. Expression level differences between WT and *Prox1* cKO lenses were determined using the EdgeR BioConductor package, using the pairwise qCML method exact test with a Benjamini–Hochberg correction.

The resulting gene list was filtered for statistical significance ($P<0.05$) and expression at greater than 2 RPKM in either *Prox1* cKO or WT lenses (Manthey et al., 2014b). Only genes with a greater than 2.5-fold difference between *Prox1* cKO and WT were considered so as to reduce false positives due to the genetic noise inherent in non-inbred mouse populations (Manthey et al., 2014b).

Bioinformatics analysis of RNA-seq data

The gene lists generated from RNA-seq were analyzed using the DAVID bioinformatics resource (Huang et al., 2009) to identify functionally related gene ontology (GO) categories ascribed to the differentially expressed genes (DEGs). Similar GO terms were grouped/clustered and assigned an enrichment score (DAVID score) to predict biological significance.

Lens-enrichment analysis by the gene prediction tool *iSyTE*

We performed two types of analysis on *Prox1* cKO lens DEGs using the *iSyTE* database. In the first, we investigated the significance of the *Prox1* cKO lens DEGs (642 genes, $P<0.05$) in lens biology by analyzing their normal expression pattern during lens development using *iSyTE* and other publically available lens expression datasets (Lachke et al., 2012). In the second analysis, we determined the proportion of genes downregulated in *Prox1* cKO lens that were among the 100 and 500 most lens-enriched genes calculated by *iSyTE*. *iSyTE* ascribes lens-enrichment scores at various embryonic and postnatal stages in lens development by performing a genome-wide expression comparison (termed '*in silico* subtraction') between microarray datasets for the lens (at stages E10.5, E11.5, E12.5, E16.5, E19.5, P0) with the embryonic whole body (WB) minus eyes reference dataset (Lachke et al., 2012; A. Kakrana and S.A.L., unpublished). The lens-enrichment score for a gene is a measure of its difference in expression [expressed as fold change (FC)] in the lens compared with the whole embryonic body reference at $P<0.05$. Both the above analyses used previously published lens microarray data (GEO datasets GSE32334, GSE47694 and GSE31643) analyzed by an in-house *Python* script (S.A.L. laboratory). The *iSyTE* lens-enrichment scores for DEGs were plotted against their RNA-seq FC. Further, the significance of the differences in lens enrichment for *Prox1* cKO upDEGs and downDEGs was estimated using a χ^2 test followed by a two-tailed *t*-test. The proportion of *Prox1* cKO DEGs in the top 500 and top 100 *iSyTE* lens-enriched genes for different lens stages (E10.5, E11.5, E12.5, E16.5, E19.5, P0) was then estimated.

Phylogenetic foot printing

Gene sequences for *Fgfr1-4*, *Fgfrl1* and *Lctl* were obtained from the human (hg38), mouse (m38.p2) and chicken (4.0, Ensembl release 78) genome assemblies. The −500 to +1 bp regions of these sequences were aligned using CLUSTAL W (Thompson et al., 1994) on the SDSC Biology WorkBench (v3.2) (Subramaniam, 1998). These regions were analyzed for the known Prox1 binding sites: 1, CA(not A)(N)(N)(C or G)(C or T); and 2, (A or C) AAG(N)(not A) (Chen et al., 2008) using PATTERNMATCH (Subramaniam, 1998) and overlaid upon the multiple sequence alignments to assess evolutionary conservation.

Chromatin immunoprecipitation

Lenses were collected from E14.5 chicken embryos, and 180 mg pooled samples were fixed for 5 min in 1% formaldehyde, flash frozen and pulverized using a Covaris CryoPREP. Nuclei were extracted and processed using the truChIP Chromatin Shearing Kit (Covaris) and chromatin sheared using a Covaris S2 adaptive focused acoustic disrupter. ChIP was carried out using 100 µg chromatin per sample, pulling down with 1 µl anti-Prox1 (Chen et al., 2008). Crosslinks were reversed and samples were analyzed by quantitative PCR. All primers are listed in Table S1. These data were normalized to 1% input (Haring et al., 2007) and were analyzed by two-way ANOVA using planned comparisons against the +5 kb region of each gene.

Rat lens explant culture

Rat lens epithelial explants were prepared as described previously (Wang et al., 2010). Explants were cultured for 5 days in the absence (control) or presence of human recombinant FGF2 (100 ng/ml; Peprotech, 1001B), and in the presence or absence of the following inhibitors: FGFR antagonist SU5402 (Sigma-Aldrich, SML0443); MEK inhibitor UO126 (Cell Signaling, 9903S); PI3K/AKT inhibitor LY294002 (Cell Signaling, 9901S). For immunofluorescence, explants were immunostained for Prox1, as above, with Hoechst (nuclear stain), and for β-catenin (Wang et al., 2010).

For western blotting, cell lysates were prepared as previously described (Zhao et al., 2015), with the addition of a phosphatase inhibitor cocktail (Roche, 04906845001). Membranes were blocked and then incubated in primary antibody, either Prox1 [1:1000 (Chen et al., 2008)] or Gapdh (1:5000; Sigma-Aldrich, G8795), overnight at 4°C, and rinsed. The membrane was then incubated with either anti-rabbit (Cell Signaling, 7074; 1:5000) or anti-mouse (Zymed, 62-6520; 1:10,000) HRP-conjugated secondary antibodies. Enhanced chemiluminescence (Millipore, WBKLS0500) was used to detect protein bands. Resultant bands from three independent experiments were captured using the ChemiDoc MP imaging system (Bio-Rad) and band intensities quantified using Image Lab software (version 4.0, Bio-Rad). Statistical significance was assessed using a non-parametric one-way ANOVA test followed by a Šídák multiple comparison post-test, with data reported as mean±s.e.m.

Acknowledgements

We thank Brewster Kingman of the University of Delaware Sequencing and Genotyping Center and Dr Shawn Polson of the University of Delaware Center for Bioinformatics and Computational Biology, for technical support of the RNA-seq experiment. We thank the staff of the University of Delaware Bioimaging facility for their excellent support of the microscopes used in this work. These core facilities are supported by grants from the NIH National Center for Research Resources [05 P20 RR016472-12], the NIH National Institute of General Medical Sciences [8 P20 GM103446-12], and National Science Foundation EPSCoR [EPS-081425].

Competing interests

The authors declare no competing or financial interests.

Author contributions

D.S.A. is the lead author and contributed to the concept and design, performed experiments and analyzed data. D.A. designed and implemented the DEG systems analysis and edited this work. T.S. performed the rat lens explant experiments. T.B.R. helped develop and perform immunohistochemistry. S.A.L. contributed to the concept and design, provided financial support, and helped design the systems analysis of DEGs, and edited the manuscript. F.J.L. contributed to the concept of this work, provided financial support, and edited the manuscript. M.K.D. is the senior author, developed the concept, revised the manuscript, and provided financial support. D.S.A., D.A., F.J.L., S.A.L. and M.K.D. wrote the manuscript and all authors read and approved the final manuscript.

Funding

This work was supported by grants from the National Institutes of Health (NIH)/National Eye Institute to M.K.D. [R01 EY012221], S.A.L. [R01 EY021505] and F.J.L. [R01 EY03177]; and grants from the Delaware Institutional Networks for Biomedical Research Excellence [GM103446]. The confocal microscope used in this study was acquired via an NIH major instrumentation grant [1S10 RR027273-01]. Deposited in PMC for release after 12 months.

Supplementary information

Supplementary information available online at
http://dev.biologists.org/lookup/suppl/doi:10.1242/dev.127860/-/DC1

References

Bassnett, S., Wilmarth, P. A. and David, L. L. (2009). The membrane proteome of the mouse lens fiber cell. *Mol. Vis.* **15**, 2448-2463.

Bhat, S. P. (2001). The ocular lens epithelium. *Biosci. Rep.* **21**, 537-563.

Bookout, A. L. and Mangelsdorf, D. J. (2003). Quantitative real-time PCR protocol for analysis of nuclear receptor signaling pathways. *Nucl. Recept. Signal.* **1**, e012.

Chen, X., Taube, J. R., Simirskii, V. I., Patel, T. P. and Duncan, M. K. (2008). Dual roles for Prox1 in the regulation of the chicken betaB1-crystallin promoter. *Invest. Ophthalmol. Vis. Sci.* **49**, 1542-1552.

Cross, M. and Dexter, T. M. (1991). Growth factors in development, transformation, and tumorigenesis. *Cell* **64**, 271-280.
Cui, W., Tomarev, S. I., Piatigorsky, J., Chepelinsky, A. B. and Duncan, M. K. (2004). Mafs, Prox1, and Pax6 can regulate chicken betaB1-crystallin gene expression. *J. Biol. Chem.* **279**, 11088-11095.
Dash, S., Dang, C. A., Beebe, D. C. and Lachke, S. A. (2015). Deficiency of the RNA binding protein caprin2 causes lens defects and features of peters anomaly. *Dev. Dyn.* **244**, 1313-1327.
de Iongh, R. U. and Duncan, M. K. (2015). Lens epithelium and posterior capsular opacification | Springer. In *Lens Epithelium and Posterior Capsular Opacification* (ed. S. Saika, L. Werner and F. J. Lovicu), pp. 81-104. Tokyo, Japan: Springer.
de Iongh, R. U., Lovicu, F. J., Chamberlain, C. G. and McAvoy, J. W. (1997). Differential expression of fibroblast growth factor receptors during rat lens morphogenesis and growth. *Invest. Ophthalmol. Vis. Sci.* **38**, 1688-1699.
Duncan, M. K., Cui, W., Oh, D.-J. and Tomarev, S. I. (2002). Prox1 is differentially localized during lens development. *Mech. Dev.* **112**, 195-198.
Duncan, M., Cvekl, A., Kantorow, M. and Piatigorsky, J. (2004). Lens crystallins. In *Development of the Ocular Lens* (ed. F. Lovicu and M. Robinson), pp. 119-150. Cambridge, UK: Cambridge University Press.
Firtina, Z., Danysh, B. P., Bai, X., Gould, D. B., Kobayashi, T. and Duncan, M. K. (2009). Abnormal expression of Collagen IV in lens activates unfolded protein response resulting in cataract. *J. Biol. Chem.* **284**, 35872-35884.
Fon Tacer, K., Bookout, A. L., Ding, X., Kurosu, H., John, G. B., Wang, L., Goetz, R., Mohammadi, M., Kuro-o, M., Mangelsdorf, D. J. et al. (2010). Research resource: Comprehensive expression atlas of the fibroblast growth factor system in adult mouse. *Mol. Endocrinol.* **24**, 2050-2064.
Fromm, L., Shawlot, W., Gunning, K., Butel, J. S. and Overbeek, P. A. (1994). The retinoblastoma protein-binding region of simian virus 40 large T antigen alters cell cycle regulation in lenses of transgenic mice. *Mol. Cell. Biol.* **14**, 6743-6754.
Goetz, R., Beenken, A., Ibrahimi, O. A., Kalinina, J., Olsen, S. K., Eliseenkova, A. V., Xu, C., Neubert, T. A., Zhang, F., Linhardt, R. J. et al. (2007). Molecular insights into the klotho-dependent, endocrine mode of action of fibroblast growth factor 19 subfamily members. *Mol. Cell. Biol.* **27**, 3417-3428.
Haring, M., Offermann, S., Danker, T., Horst, I., Peterhansel, C. and Stam, M. (2007). Chromatin immunoprecipitation: optimization, quantitative analysis and data normalization. *Plant Methods* **3**, 11.
Harvey, N. L., Srinivasan, R. S., Dillard, M. E., Johnson, N. C., Witte, M. H., Boyd, K., Sleeman, M. W. and Oliver, G. (2005). Lymphatic vascular defects promoted by Prox1 haploinsufficiency cause adult-onset obesity. *Nat. Genet.* **37**, 1072-1081.
Hawse, J. R., DeAmicis-Tress, C., Cowell, T. L. and Kantorow, M. (2005). Identification of global gene expression differences between human lens epithelial and cortical fiber cells reveals specific genes and their associated pathways important for specialized lens cell functions. *Mol. Vis.* **11**, 274-283.
Huang, D. W., Sherman, B. T. and Lempicki, R. A. (2009). Systematic and integrative analysis of large gene lists using DAVID bioinformatics resources. *Nat. Protoc.* **4**, 44-57.
Johnson, N. C., Dillard, M. E., Baluk, P., McDonald, D. M., Harvey, N. L., Frase, S. L. and Oliver, G. (2008). Lymphatic endothelial cell identity is reversible and its maintenance requires Prox1 activity. *Genes Dev.* **22**, 3282-3291.
Kim, J. I., Li, T., Ho, I.-C., Grusby, M. J. and Glimcher, L. H. (1999). Requirement for the c-Maf transcription factor in crystallin gene regulation and lens development. *Proc. Natl. Acad. Sci. USA* **96**, 3781-3785.
Kurose, H., Okamoto, M., Shimizu, M., Bito, T., Marcelle, C., Noji, S. and Ohuchi, H. (2005). FGF19-FGFR4 signaling elaborates lens induction with the FGF8-L-Maf cascade in the chick embryo. *Dev. Growth Differ.* **47**, 213-223.
Kurosu, H., Choi, M., Ogawa, Y., Dickson, A. S., Goetz, R., Eliseenkova, A. V., Mohammadi, M., Rosenblatt, K. P., Kliewer, S. A. and Kuro-o, M. (2007). Tissue-specific expression of betaKlotho and fibroblast growth factor (FGF) receptor isoforms determines metabolic activity of FGF19 and FGF21. *J. Biol. Chem.* **282**, 26687-26695.
Lachke, S. A., Alkuraya, F. S., Kneeland, S. C., Ohn, T., Aboukhalil, A., Howell, G. R., Saadi, I., Cavallesco, R., Yue, Y., Tsai, A. C.-H. et al. (2011). Mutations in the RNA granule component TDRD7 cause cataract and glaucoma. *Science* **331**, 1571-1576.
Lachke, S. A., Ho, J. W. K., Kryukov, G. V., O'Connell, D. J., Aboukhalil, A., Bulyk, M. L., Park, P. J. and Maas, R. L. (2012). iSyTE: integrated systems tool for eye gene discovery. *Invest. Ophthalmol. Vis. Sci.* **53**, 1617-1627.
Lengler, J., Krausz, E., Tomarev, S., Prescott, A., Quinlan, R. A. and Graw, J. (2001). Antagonistic action of Six3 and Prox1 at the gamma-crystallin promoter. *Nucleic Acids Res.* **29**, 515-526.
Li, H., Tao, C., Cai, Z., Hertzler-Schaefer, K., Collins, T. N., Wang, F., Feng, G.-S., Gotoh, N. and Zhang, X. (2014). Frs2α and Shp2 signal independently of Gab to mediate FGF signaling in lens development. *J. Cell Sci.* **127**, 571-582.
Lovicu, F. J. and McAvoy, J. W. (2005). Growth factor regulation of lens development. *Dev. Biol.* **280**, 1-14.
Lovicu, F. J., McAvoy, J. W. and de Iongh, R. U. (2011). Understanding the role of growth factors in embryonic development: insights from the lens. *Philos. Trans. R. Soc. Lond. B Biol. Sci.* **366**, 1204-1218.
Mamuya, F. A., Wang, Y., Roop, V. H., Scheiblin, D. A., Zajac, J. C. and Duncan, M. K. (2014). The roles of alphaV integrins in lens EMT and posterior capsular opacification. *J. Cell. Mol. Med.* **18**, 656-670.
Manthey, A. L., Lachke, S. A., FitzGerald, P. G., Mason, R. W., Scheiblin, D. A., McDonald, J. H. and Duncan, M. K. (2014a). Loss of Sip1 leads to migration defects and retention of ectodermal markers during lens development. *Mech. Dev.* **131**, 86-110.
Manthey, A. L., Terrell, A. M., Lachke, S. A., Polson, S. W. and Duncan, M. K. (2014b). Development of novel filtering criteria to analyze RNA-sequencing data obtained from the murine ocular lens during embryogenesis. *Genom. Data* **2**, 369-374.
McAvoy, J. W. and Chamberlain, C. G. (1989). Fibroblast growth factor (FGF) induces different responses in lens epithelial cells depending on its concentration. *Development* **107**, 221-228.
Nakayama, Y., Miyake, A., Nakagawa, Y., Mido, T., Yoshikawa, M., Konishi, M. and Itoh, N. (2008). Fgf19 is required for zebrafish lens and retina development. *Dev. Biol.* **313**, 752-766.
Nishiguchi, S., Wood, H., Kondoh, H., Lovell-Badge, R. and Episkopou, V. (1998). Sox1 directly regulates the gamma-crystallin genes and is essential for lens development in mice. *Genes Dev.* **12**, 776-781.
Pan, H. and Griep, A. E. (1994). Altered cell cycle regulation in the lens of HPV-16 E6 or E7 transgenic mice: implications for tumor suppressor gene function in development. *Genes Dev.* **8**, 1285-1299.
Piatigorsky, J. (1975). Lens cell elongation in vitro and microtubules. *Ann. N. Y. Acad. Sci.* **253**, 333-347.
Reed, N. A., Oh, D. J., Czymmek, K. J. and Duncan, M. K. (2001). An immunohistochemical method for the detection of proteins in the vertebrate lens. *J. Immunol. Methods* **253**, 243-252.
Robinson, M. L. (2006). An essential role for FGF receptor signaling in lens development. *Semin. Cell Dev. Biol.* **17**, 726-740.
Scata, K. A., Bernard, D. W., Fox, J. and Swain, J. L. (1999). FGF receptor availability regulates skeletal myogenesis. *Exp. Cell Res.* **250**, 10-21.
Schlessinger, J., Plotnikov, A. N., Ibrahimi, O. A., Eliseenkova, A. V., Yeh, B. K., Yayon, A., Linhardt, R. J. and Mohammadi, M. (2000). Crystal structure of a ternary FGF-FGFR-heparin complex reveals a dual role for heparin in FGFR binding and dimerization. *Mol. Cell* **6**, 743-750.
Shaham, O., Smith, A. N., Robinson, M. L., Taketo, M. M., Lang, R. A. and Ashery-Padan, R. (2009). Pax6 is essential for lens fiber cell differentiation. *Development* **136**, 2567-2578.
Shin, J. W., Min, M., Larrieu-Lahargue, F., Canron, X., Kunstfeld, R., Nguyen, L., Henderson, J. E., Bikfalvi, A., Detmar, M. and Hong, Y.-K. (2006). Prox1 promotes lineage-specific expression of fibroblast growth factor (FGF) receptor-3 in lymphatic endothelium: a role for FGF signaling in lymphangiogenesis. *Mol. Biol. Cell* **17**, 576-584.
Silva, P. N., Altamentova, S. M., Kilkenny, D. M. and Rocheleau, J. V. (2013). Fibroblast growth factor receptor like-1 (FGFRL1) interacts with SHP-1 phosphatase at insulin secretory granules and induces beta-cell ERK1/2 protein activation. *J. Biol. Chem.* **288**, 17859-17870.
Steinberg, F., Zhuang, L., Beyeler, M., Kälin, R. E., Mullis, P. E., Brändli, A. W. and Trueb, B. (2010). The FGFRL1 receptor is shed from cell membranes, binds fibroblast growth factors (FGFs), and antagonizes FGF signaling in Xenopus embryos. *J. Biol. Chem.* **285**, 2193-2202.
Streit, A. (2004). Early development of the cranial sensory nervous system: from a common field to individual placodes. *Dev. Biol.* **276**, 1-15.
Subramaniam, S. (1998). The Biology Workbench—a seamless database and analysis environment for the biologist. *Proteins* **32**, 1-2.
Thompson, J. D., Higgins, D. G. and Gibson, T. J. (1994). CLUSTAL W: improving the sensitivity of progressive multiple sequence alignment through sequence weighting, position-specific gap penalties and weight matrix choice. *Nucleic Acids Res.* **22**, 4673-4680.
Tomarev, S. I., Sundin, O., Banerjee-Basu, S., Duncan, M. K., Yang, J.-M. and Piatigorsky, J. (1996). Chicken homeobox gene Prox1 related to Drosophila prospero is expressed in the developing lens and retina. *Dev. Dyn.* **206**, 354-367.
Wang, Q., Stump, R., McAvoy, J. W. and Lovicu, F. J. (2009). MAPK/ERK1/2 and PI3-kinase signalling pathways are required for vitreous-induced lens fibre cell differentiation. *Exp. Eye Res.* **88**, 293-306.
Wang, Q., McAvoy, J. W. and Lovicu, F. J. (2010). Growth factor signaling in vitreous humor–induced lens fiber differentiation. *Invest. Ophthalmol. Vis. Sci.* **51**, 3599-3610.
Weber, G. F. and Menko, A. S. (2006a). Actin filament organization regulates the induction of lens cell differentiation and survival. *Dev. Biol.* **295**, 714-729. United States.
Weber, G. F. and Menko, A. S. (2006b). Phosphatidylinositol 3-kinase is necessary for lens fiber cell differentiation and survival. *Invest. Ophthalmol. Vis. Sci.* **47**, 4490-4499.
Wigle, J. T. and Oliver, G. (1999). Prox1 function is required for the development of the murine lymphatic system. *Cell* **98**, 769-778.
Wigle, J. T., Chowdhury, K., Gruss, P. and Oliver, G. (1999). Prox1function is crucial for mouse lens-fibre elongation. *Nat. Genet.* **21**, 318-322.

Development (2016) 143, 318-328 doi:10.1242/dev.127860

Zhang, P., Wong, C., DePinho, R. A., Harper, J. W. and Elledge, S. J. (1998). Cooperation between the Cdk inhibitors p27(KIP1) and p57(KIP2) in the control of tissue growth and development. *Genes Dev.* **12**, 3162-3167.

Zhao, H., Yang, Y., Rizo, C. M., Overbeek, P. A. and Robinson, M. L. (2004). Insertion of a Pax6 consensus binding site into the alphaA-crystallin promoter acts as a lens epithelial cell enhancer in transgenic mice. *Invest. Ophthalmol. Vis. Sci.* **45**, 1930-1939.

Zhao, H., Yang, T., Madakashira, B. P., Thiels, C. A., Bechtle, C. A., Garcia, C. M., Zhang, H., Yu, K., Ornitz, D. M., Beebe, D. C. et al. (2008). Fibroblast growth factor receptor signaling is essential for lens fiber cell differentiation. *Dev. Biol.* **318**, 276-288.

Zhao, G., Wojciechowski, M. C., Jee, S., Boros, J., McAvoy, J. W. and Lovicu, F. J. (2015). Negative regulation of TGFbeta-induced lens epithelial to mesenchymal transition (EMT) by RTK antagonists. *Exp. Eye Res.* **132**, 9-16.